Metal recovery from Li-ion battery waste

Technical report: Metal recovery from Li-ion battery waste

BLADERGROEN, B.J, PETRIK, L., TAWONEZVI, T., MASSIMA, E.S.M. & TSHISANO, M.

Waste Research Development and
Innovation Roadmap Research Report

29 May 2024

science & innovation
Department:
Science and Innovation
REPUBLIC OF SOUTH AFRICA

UNIVERSITY of the
WESTERN CAPE

DOCUMENT CONTROL

Degree of Confidentiality:	Public
Title:	Metal recovery from Li-ion battery waste
Author(s):	BLADERGROEN, B.J, PETRIK, L., TAWONEZVI, T., MASSIMA, E.S.M. & TSHISANO, M.
Date of Issue:	June 2024
Grant Holder:	Prof BJ Bladergroen
Organization Report Number:	CSIR/BEI/WRIU/2021/052
Prepared by:	CSIR Natural Resources and the Environment PO Box 395, Pretoria, South Africa, 0001
Prepared for:	Department of Science and Innovation Directorate Environmental Services and Technologies Private Bag X894, Pretoria, South Africa, 0001
Contract Number:	CSIR/BEI/WRIU/2015/012
Keywords:	LiB Waste, job creation, extraction technology development
Version:	Final

REVIEWED BY:		
Responsibility:	Name:	Organization:
Internal Reviewer:		
External Reviewer:		

APPROVED BY (On behalf of issuing organisation):		
Name:	Position:	Date:

EXECUTIVE SUMMARY

The research described in this report explores the recovery of nickel (Ni) and cobalt (Co) from spent lithium-ion batteries (Li-ionBs) through a hydro-electrometallurgy process, aiming to facilitate closed-loop recycling of Li-ionB cathode materials. The innovative approach combines hydrometallurgy and potentiostatic electrometallurgy, bypassing traditional, energy-intensive purification methods such as solvent extraction, selective precipitation, and ion exchange.

Key leaching parameters—including solid/liquid ratio, temperature, acid and oxidant concentration, and leaching time—were optimized to achieve over 94% recovery of Ni, Co, manganese (Mn), and lithium (Li) from LiN0.5Mn0.3Co0.2O2 (NMC 532) cathode material, with the resultant products boasting a minimum purity of 98%. Electrowinning parameters like applied potential, temperature, pH, buffer concentrations, and cathode rotational speed were fine-tuned to recover a $Ni_{0.65}Co_{0.35}$ composite at a rate of 0.060 g/cm^2/hr with 88% current efficiency. The Ni-Co composite was subsequently processed with H_2SO_4 to yield $NiSO_4$-$CoSO_4$ salt with a 99% yield. These results confirm the technical feasibility of high-purity, industrial-grade Ni-Co composite recovery. Additionally, valuable by-products such as Li_2CO_3 and $Mn(OH)_2$ were extracted from spent electrolytes through chemical precipitation.

Furthermore, the study employed electrospun polyethylene terephthalate (PET) functionalized with Di-2-ethylhexyl phosphoric acid (DEHPA) to recover metal ions (Ni, Co, or Mn) from spent LIB cathode materials. Optimal metal adsorption conditions—contact time and pH—were determined, and the performance of the pristine and modified adsorbent (PET-DEHPA) was characterized using FTIR, XPS, SEM, EDS, TGA, and XRD. The optimal conditions for metal ion adsorption were found to be pH 4, 60 minutes of contact time, and an initial metal ion concentration of 100 mg/L. Experimental results indicated a recovery efficiency of 57% for Mn ions, significantly higher than that for Ni (7%) and Co (13%). Mn ion adsorption was rapid, occurring within 60 minutes, and showed selectivity over Ni and Co ions. The PET-DEHPA nanofiber adsorbent also demonstrated excellent regeneration capability over five cycles, underscoring its economic viability and sustainability.

Overall, this study introduces a promising method for recycling Mn ions from spent LIBs, highlighting both the technical feasibility and the economic potential of the proposed processes.

TABLE OF CONTENTS

1 Description of Research Topics

This project aimed at recovering valuable metals from Li-ion battery waste. This goal was achieved using two principal methods including galvanostatic electrowinning process and adsorption separation protocol. Therefore, the following technical report overviews optimisation of Co and Ni Electrowinning process followed by the development of a comprehensive hydro-electrometallurgy recycling process, and the recovery of metals from spent electrowinning electrolytes using Na and Non-Na systems. The second section of the report covers production of functionalized polyethylene terephthalate nanofibers for the adsorption recovery of precious metals from synthetic spent LIBs mixtures. The research outputs from these headlines are also outlined.

1.1 Selective Recovery of Valuable Cobalt-Nickel Alloys and Inorganic Compounds from Spent Lithium Ion Battery Cathodes for Open and Closed Loop Recycling (PhD Thesis)

1.1.1 Background

Lithium-ion batteries (Li-ionBs) have been extensively deployed as the electrochemical power source in various portable electronic devices, energy storage systems, and electric vehicles (Njema et al., 2024). Over the years, Li-ionBs have been the battery technology with the highest development, production, and demand in the last decade, and their market has been extrapolated to draw in 116 billion USD by 2030 (ESMAP, 2022). Subsequently, a considerable number of spent Li-ionBs are disposed of as waste extrapolated annually. The current processes utilised for recycling spent Li-ionB entail high-cost, energy-intensive, and eco-hazardous processes and materials (Milian et al., 2024). This results in only a mere 5% of spent Li-ionBs currently being recycled (Tawonezvi et al., 2023). The continued employment of such processes could lead to the hindrance of Li-ionBs development and production. Therefore, the development of an effective, low-cost, low-energy intensive, and eco-friendly recycling process route for recovering precious metals (i.e., Li, Co, Ni, and Mn) is imperative and imminent.
The cathode of Li-ionBs is the most determinant component for the battery's electrochemical performance (Liu et al., 2016). This is also the most valuable component because it contains significant amounts of highly valuable metals such as Li, Co, Ni, and Mn (Milian et al., 2024). Notably, Ni and Co are significantly more valuable than Li and Mn. Conventionally, battery metals are selectively recovered as their metal solutions from complex multi-ion leachate solutions by using solvent extraction, ion exchange, and selective precipitation (Tawonezvi., 2024). The solid metal deposit is then obtained using galvanostatic electrowinning as the process to reduce metal ions to their metallic solid state. In this work, Ni-Co alloys from spent Li-ionBs were selectively recovered from leachate solutions that contain Li, Mn, Co, and Ni ions through potentiostatic electrowinning. Since the post electrowinning spent liquor still constitutes low traces of Ni and Co and significant amounts of Li and Mn, additional Na-based chemical precipitation unit operation was added to recover $NMC(OH)_2$, $Mn(OH)_2$, and Li_2CO_3 materials.

The rationale of this research is hinged on the elimination of cost and energy-intensive hydrometallurgy intermediate processes like solvent extraction, ion exchange, and selective precipitation (to extract Ni and Co selectively), utilisation of potentiostatic techniques (instead of conventional galvanostatic technique) to selective extract specific metals and enhance the purity, integration of rotating cathodes to increase deposition rate and utilisation of Pt coated Ti dimensionally stable anodes (DSA) to reduce deposit contamination and consequently levelized cost of operation. It is believed that through applying constant potential applicable for Co and Ni reduction reactions (potentiostatic electrowinning), valuable Ni and Co can be selectively separated from less valuable Li and Mn. The elimination of intermediate purification stages is based on the fact that the Co and Ni salts or pure Ni and Co compounds are introduced to the cathode synthesis or production process as a mixture; therefore, there is no need to separate them beforehand. Recovered Ni-Co alloys are used as the feedstock for NMC cathode production processes.

1.1.2 Methodology and Results: Leaching

Firstly, this research illustrates the applicability of inorganic acid-reductant leachant-based leaching of NMC 532 to effectively dissolute and recover all valuable metals in the cathode material. This approach provides quantitative recovery data for each element of the entire particle population at different operational parameters: reductant and inorganic acid concentration, S/L ratio, reaction time, and temperature. The quantification of elemental recovery data was done through ICP-OES using separate elemental standards for each metal to increase the data's accuracy. EDS was also used to support ICP-OES composition data. Phase composition was assessed through XRD analysis. Morphology and particle size were analysed using HR-SEM. Through utilisation of leachant solutions comprising 2M H_2SO_4 + 6 vol.% H_2O_2, and a 75 g/L S/L ratio and conducting leaching for 20 minutes (to free aluminium foil and carbon flakes from cathode matrix) and 120 minutes (to leach active metals) at a temperature of 60°C, peak leaching recovery efficiency of 98.1% for Li, 97.1% for Co, 96.1% for Ni, and 95.7% for Mn were attained. The maximum metal recovery that was attained is 0.595 $g_{total\ metal}/g_{cathode}$.

1.1.3 Methodology and Results: Selective Electrowinning

Secondly, the effects of key electrowinning parameters were quantified and studied, and alternative electrodes to suppress the extent of scaling, electrode resistivity, operational and capital costs and life cycle duration limitation were tested. This study was done using synthetic Ni, Co, Mn and Li sulphate solutions mimicking the NMC 532 ratio of elements. This quasi-model is done to elucidate the effect of multiple influencing parameters, through isolation and varying, on the selective electrodeposition of Co-Ni from multi-ion (Li, Ni, Mn and Co) complex solutions before applying it using real cathode leachates. The key parameters for electrowinning studied were applied potential, metal ion concentration, pH, temperature, rotating cathode speed, Na_2SO_4 dosage and buffer dosage. The optimal level of each leaching operational parameter was established and noted for the next experimental phase. In the second phase of experiments, electrowinning of Ni-Co composite from NMC 532 sulphate solutions was investigated in a laboratory cell equipped with electrodes of the same size and design. Most of the electrowinning analysis was done on the electrodeposition of Co-Ni composite on cost-effective and highly electroconductive Al alloy cathodic plates and highly electroconductive, long-life cycle and low levelized-cost of operation electroconductive Pt-coated Ti anodes.

The cathodic deposition of Ni-Co composite material was accelerated at high applied potential, high pH, high active surface area, low inter-electrode distance, high metal ion concentration

and high temperature. Anode scaling at optimal electrowinning conditions was inhibited when Al cathodes were coupled with Pt-Coated Ti anodes. Due to the presence of the platinum film, the titanium electrode was not passivated. The electrowinning parameters applied potential, temperature, pH, Co-Ni, Na_2SO_4 and buffer concentration, and electrode distance and active area were successfully optimised to recover $Ni_{0.65}Co_{0.35}$ at a minimum rate of 0.06 g/cm^2.hr at 88% current efficiency. 90 % of the Co and 77 % of the Ni in the leachate was recovered in a 3 h electrowinning run. 5.8 g of Ni-Co alloy was obtained per 18.75 g of NMC 532 cathode. The optimum process conditions that yielded 98 % Ni-Co purity, 88% current efficiency and ideal deposit cohesion for Ni-Co deposition were: conditions (-1.15 V vs Ag/AgCl, 30 g/L Co-Ni, 50 °C, 15 g/L of Na_2HPO_4, 15 g/L Na_2SO_4 and pH 4.5).

Following several tests with synthetic solutions, electrowinning was then accomplished using the real NMC 532 solution obtained after the leaching of cathode material from spent Li-ionBs. The best parameters for deposition were defined in the Co-Ni electrowinning optimisation experiments. However, as the purification stage was not entirely effective in the removal of all contaminants, especially Mn, the obtained deposit was relatively high albeit somehow below ideal standards; it constituted predominantly amorphous $Ni_{0.7}Co_{0.3}$ powder with purity of over 97.35 %. The $Ni_{0.7}Co_{0.3}$ composite was reacted with 2M H_2SO_4 for 3 h when contacted at 75 g/L to produce $NiSO_4$-$CoSO_4$ salt at 99% yield for the hydrous NMC production plants. The anhydrous NMC production plants can utilise the recovered pure Ni-Co powder.

1.1.4 Methodology and Results: Precipitation

In the last phase of the experiments, the metals remaining in the spent electrolyte from the electrowinning were recovered through multi-stage precipitation to recover $Mn(OH)_2$ and Li_2CO_3 and hydroxide composite formulation of Ni, Mn and Co ($(NMC(OH)_2$) at over 98 % precipitation efficiency. The key parameters for pH-based precipitation were temperature and pH. The optimal levels of each leaching operational parameter were established and noted. The pH of the spent electrolyte is adjusted to levels 7.8 and 12.8 using NaOH to extract $Ni_xMn_yCo_z(OH)_2$ and $Mn(OH)_2$, respectively. The optimal temperature was adjusted to 20 ^{0}C, reaction time to 60 mins and agitation speed to 300 rpm. The key parameters for chemical-based precipitation of Li_2CO_3 recovery were temperature, CO_2^{-3} to Li ratio and pH. The optimal levels of each leaching operational parameter were established and noted. The pH of the spent electrolyte is adjusted to level 13.5, CO_3^{2-} to Li ratio to 1.6:1 and temperature to 20 ^{0}C, reaction time to 60 mins and agitation speed to 500 rpm to extract more than 95 % Li in the resultant solution as Li_2CO_3. The recycling cost (R/kg) of cathode was calculated to be R 153/kg which is at least 50 % lesser than R 360/kg, R 308/kg and R 258/kg recycling costs for direct recycling, pyrometallurgical and hydrometallurgical processes respectively.

1.1.5 Process Overview

A small fraction of the process resultant solution from the integrated leaching-electrowinning-precipitation overall process is recycled for use in the leachate pH adjustment stage, the majority portion is discarded as per National Environmental Protection Agency (NEPA) regulations since it contains negligible and environmentally tolerant metal concentrations. The obtained results demonstrate the feasibility of a semi-closed loop spent Li-ionB cathode recycling process comprising of battery pre-treatment, single-stage leaching, single-compartment electrowinning cell, precipitation reactor and sulphation reactor. The main objective of this work, Ni-Co composite recovery, was successfully reached since the deposit

chemical composition presents a rather high purity of Ni-Co composite, i.e., 98 wt. % (1.9 % Mn), at a relatively higher rate of at least 0.06 g/hr.cm^2 and moderate recycling cost of R 153 (US$ 7/kg) of NMC cathode.

The Ni-Co composite recovered from spent Li-ionBs was targeted for closed and open loop recycling since besides Li-ionB cathode production, which is the main target use for the Ni-Co composite, Ni-Co alloys and alloys can also be used production of magnetic films, electrocatalysis materials, electronic chips, anti-corrosion systems, micro and nanogears among other various technological applications that require pure Ni-Co alloys (98 wt. %). The recovered Li_2CO_3 is a versatile compound with applications ranging from production of Li-ionBs, stabilizing mood in pharmaceuticals to enhancing properties in glass and ceramics, aluminium production, metallurgical processes, chemical synthesis, and absorption refrigeration systems for air conditioning. The recovered $Mn(OH)_2$ can be employed as a coagulant in water treatment, a cathode material in alkaline batteries, and a micronutrient supplement in agriculture, showcasing its versatility across applications. Lastly, the recovered hydroxide composite formulation of Ni, Mn and Co ($NMC(OH)_2$) is to be used solely for Li-ionB cathode production.

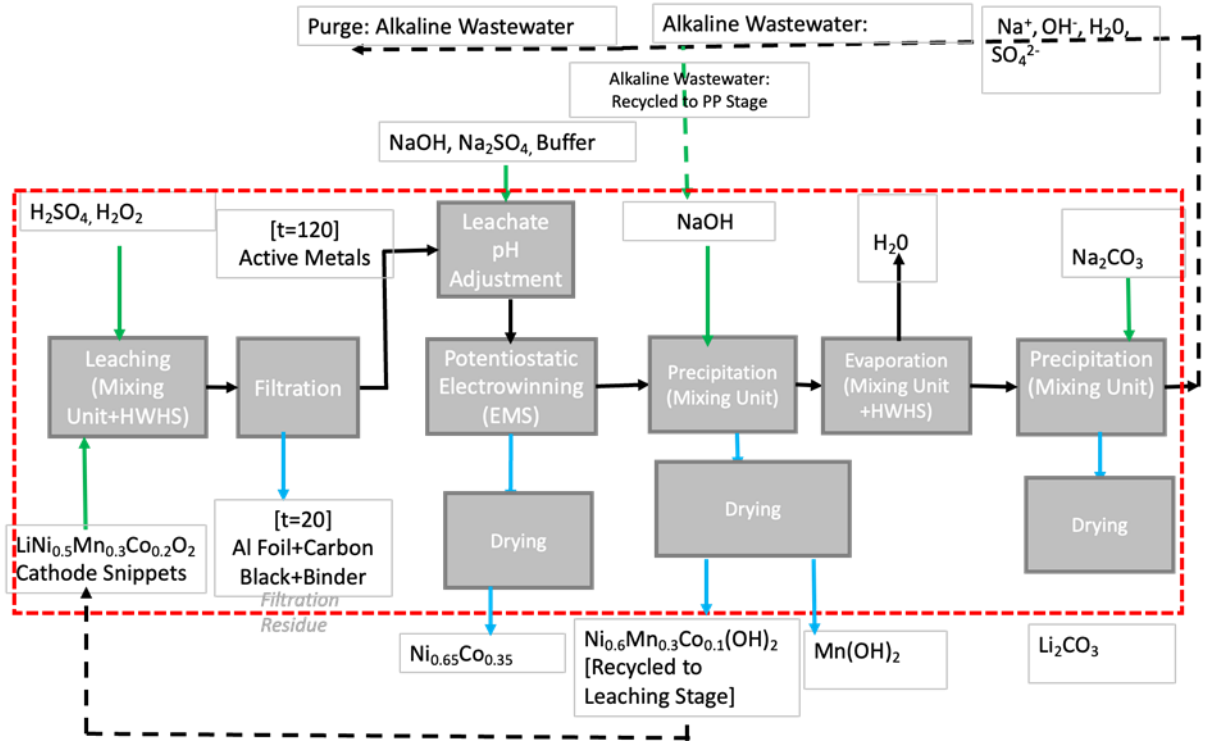

Figure 1: Graphical abstract of the valuable Ni-Co and metallic by products recovery process

1.2 Metal Recovery Using Functionalized Polyethylene Terephthalate Nanofibers (MSc study)

1.2.1 Background

The escalating demand for consumer electronics and electric vehicles (EVs) has fueled a significant increase in the consumption of lithium-ion batteries (LIBs) (Tawonezvi et al. 2023).

According to statistics, the lifetime of LIBs in digital products is only one to three years, and the lifetime of LIBs in power vehicles is five to eight years (Zeng et al. 2012; Zheng et al. 2018). Spent LIBs have a high economic value because they contain a significant number of valuable metals, some with an even higher grade than the metal grade in natural ores [3]. Valuable metals such as Li, Ni, Co and Mn from spent LIBs bring significant economic benefits if they can be recycled. The recycling of these metals has become imperative due to the environmental crisis and resource scarcity associated with the lack of eco-friendly recycling methods (Chen and Ho, 2018). Pyrometallurgy and hydrometallurgy are the two prominent recycling methods that have been employed to recover valuable metals from spent LIBs. Pyrometallurgy is energy-intensive nature and Li is usually lost in the slag phase (Zheng et al. 2018). Hydrometallurgy, particularly the liquid-liquid extraction (LLE) method, has emerged as the predominant choice instead. However, LLE's extensive use of organic solvents and its multi-step process compromise the recovery efficiency of metals and result in substantial waste production (Gao et al. 2022). In response, a promising alternative method involves an adsorption process whereby nanofibers are employed as adsorbents due to their high surface area, customizable surface properties and thus, selectivity towards metal ions (Ligneris et al. 2020).

The electrospinning technique has gained much interest in the fabrication of nanofibers due to its versatility in spinning a wide variety of polymeric fibers and ability to consistently produce fibers in the submicron range that is otherwise difficult to achieve by using standard mechanical fiber-spinning techniques (Bhardwaj and Kundu, 2010). Amongst other polymers, polyethylene terephthalate (PET) has been successfully electrospun into nanofibers for the recovery of metal ions (Totito et al. 2021). However, introducing functional ligands into these PET nanofibers was found enhancing the adsorption capacity (Khorram et al. 2017). Owing to its advantages such as durability, thermal stability, chemical resistance (Thamer et al. 2019) and recyclability (Abbas et al. 2018), PET has been used as a support in numerous adsorption studies. Martin et al. (2017) synthesized aminated PET nanofiber adsorbent which achieved a maximum Pb^{2+} adsorption capacity of 50 mmol/g after 30 mins. In another study by Pereao et al., (2021), PET nanofibers were functionalized with diglycolic anhydride (DGA) ligand, and the adsorption capacity was increased to 135 and 123 mg/g for Ce^{3+} and Nd^{3+}, respectively compared to pristine PET nanofibers. They further showed these PET-DGA nanofibers demonstrated a good selectivity for Ce^{3+} in the presence of competing ions like Sr^{2+}, Ni^{2+} and Co^{2+} ions. Khorram et al., (2019) functionalized PET with chitosan through cold plasma technique for adsorption of Cr^{4+}. The obtained PET nanofibers demonstrated a higher adsorption capacity of 110 mg/g at pH of 4 compared to pristine PET nanofibers (Khorram et al. 2017). Organic ligands, such as DEHPA ligand has been widely used in liquid-liquid extraction and solid liquid extraction for recovery and separation of metal ions (Chen and Ho, 2017, Tarus et al. 2017). Nunes da Silva et al. (2019) found that nylon-6 nanofibers functionalized with DEHPA were selective for Zn^{2+} (86 %) over Ni^{2+} (5 %). Although several studies have focused on the functionalization of PET for the recovery of metal ions from solutions, only a few studies have looked at its modification with DEHPA for the potential recovery and selective adsorption of valuable metals such as Co^{2+}, Ni^{2+} and Mn^{2+} which are present in spent LIBs. This study therefore intends to fabricate functionalized PET-DEHPA nanofibers using electrospinning technique for recovery and separation of metal ions from solutions.

1.2.2 Methodology and Results: Electrospinning parameters and fabrication of nanofibers

The fabrication of PET nanofibers was performed by optimizing the electrospinning parameters including PET polymer concentration investigated was within the range of 5–20 wt%, solution flow rate (0.4–1.0 mL), collecting distance (13–20 cm) and an applied voltage of 30 kV. PET-DEHPA nanofibers were fabricated using 10 wt% (PET) dissolved in 10 mL TFA for 6 hours. Pure liquid DEHPA chelating ligand was added into the solution (5–20 %, v/v) and stirred overnight. The obtained solution was electrospun using electrospinning technique and the nanofibers were characterized by SEM, EDS, XPS, FTIR-ATR, TGA and XRD.
The optimized electrospinning parameters (10 wt%, 1.0 mL/h and 15 cm) previously obtained for pristine PET nanofibers were used to fabricate the modified PET-DEHPA nanofibers. The effect of DEHPA ligand concentration upon the surface morphology and the diameter distribution of electrospun nanofibers was evaluated. As shown in Fig. 2a, pristine PET nanofibers exhibited a non-woven and bead-free fiber morphology with an average diameter of 132 ± 52 nm. The modification of PET nanofibers with DEHPA ligand resulted in changes in the surface morphology of the nanofibers. The use of the lowest concentration of DEHPA ligand as exhibited in Fig. 2b resulted in nanofibers crosslinking, forming some beads on the fibers, and an increase in diameter to 176 ± 71 nm.

Further increase in DEHPA ligand concentrations resulted in significant crosslinking of nanofibers. This cross-linking implies the increase in durability of the produced nanofibers as the DEHPA ligand concentration increased up to 15 wt%. This effect was also reported by [18]. The average diameter further increased to 215 ± 91 nm for PET-DEHPA (Fig. 2c) but decreased to 147 ± 45 nm for PET-DEHPA (Fig. 2d). Excessive use of the DEHPA ligand led to a distinct change from nanofiber structural aspect to a nonfibrous material (Fig. 4e). Such structure could subsequently reduce some performances of PET-DEHPA nanofibers due to loss of nanofibers (Tarus et al. 2016). Following the surface characterization of the nanofibers, the elemental analysis of the nanofibers was conducted using EDS to determine the amount of DEHPA ligand incorporated into the PET nanofibers after the blending process. Fig. 2g shows the percentages of phosphorous (P) atom which are regarded as the representative of the amount of DEHPA ligand present in the PET-DEHPA nanofibers. The percentage of P within the samples increased from 3.8 % up to 16.3 % and the amounts directly correlated with the blended amounts of DEHPA (C1:5 %, C2:10 %, C3:15 % and C4:20 %) ligand into PET in TFA solution

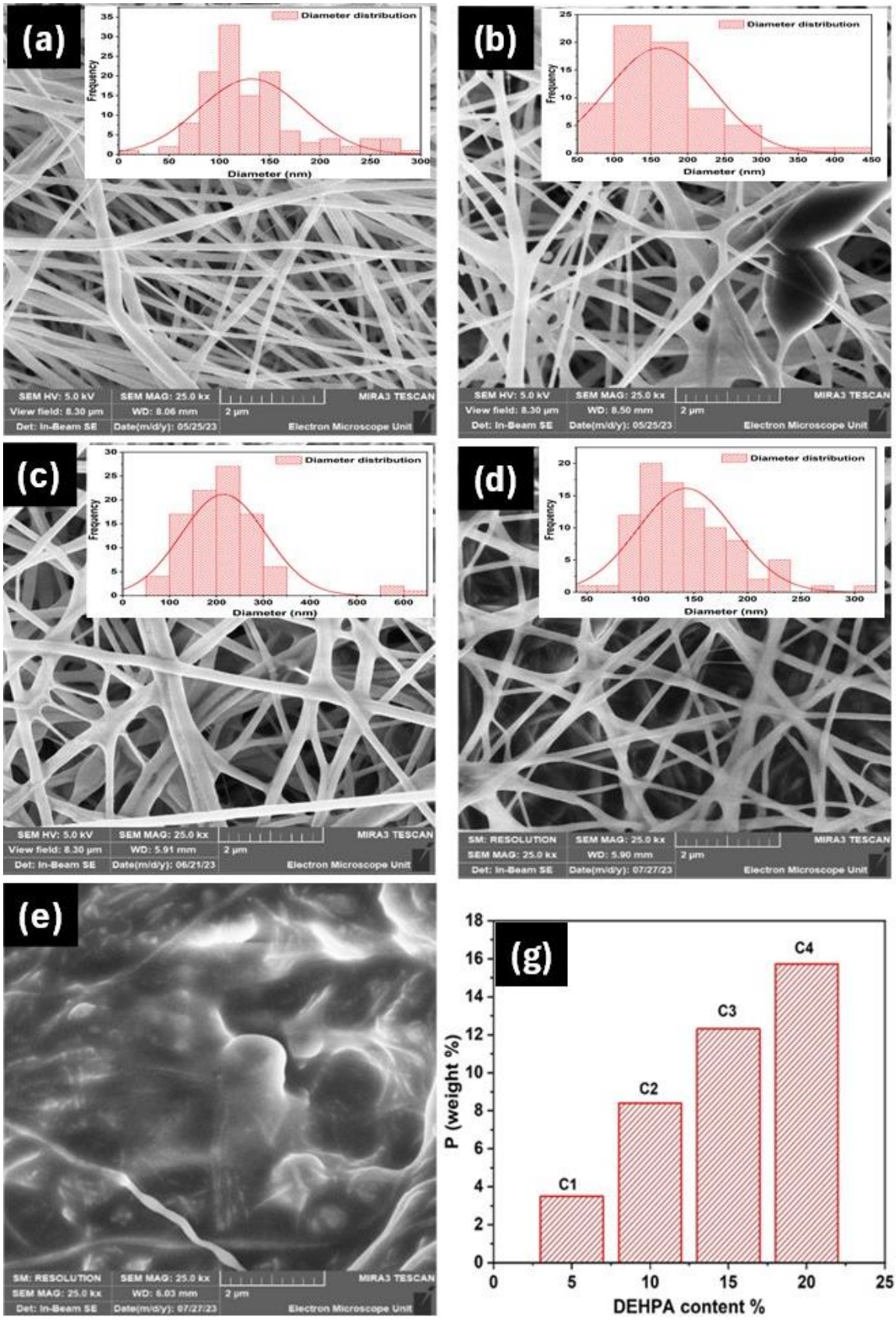

Figure 2: SEM micrographs and diameter distributions of (a): Pristine PET nanofibers and modified PET nanofibers at (b): 5 wt%, (c): 10 wt%, (d): 15 wt%, (e): 20 wt% of DEHPA ligand. (g): Phosphorous content by EDS analysis of PET-DEHPA nanofibers.

Since EDS is a semiquantitative technique, XPS was used to further confirm the elemental analysis data. Table 1 shows the elemental percentages as depicted from XPS analysis.

Table 1: XPS elemental analysis of PET-DEHPA nanofibers

Elements	PET-DEHPA nanofibers			
	(5 wt%)	(10 wt%)	(15 wt%)	(20 wt%)
P	2.92	3.62	4.47	5.04
O	21.96	19.56	19.99	19.98
C	74.89	76.56	75.04	74.11
Al	0.24	0	0	0.82
Ca	0	0.26	0.37	0
Na	0	0	0.14	0.05

It was found that the contents of C (72–77 %) and O (~ 20 %) were almost the same in all PET-DEHPA nanofibers. As expected, P content increased with the increase in the amount of DEHPA ligand used during the synthesis process. Therefore, the XPS data improved on the quantitative evaluation compared to EDS data. The other elements, Al, Ca and Na were only detected in insignificantly small amounts, less than 1 %. Fig. 3a shows that the decomposition process of PET nanofibers occurred in a single step (365 °C) while PET-DEHPA nanofibers all showed a two-step degradation process. The first step was at about 230 °C which was attributed to the degradation of DEHPA chemical compounds, and the other step was at about 360 °C which was then attributed to the degradation of PET chemical compounds. These findings were in good agreement with Singh et al. (2013) and Yadav et al. (2013) whose investigations showed that the decomposition of DEHPA occurred between 200 and 300 °C while that of PET according to Pereao et al. (2021) was found at a temperature above 300 °C.

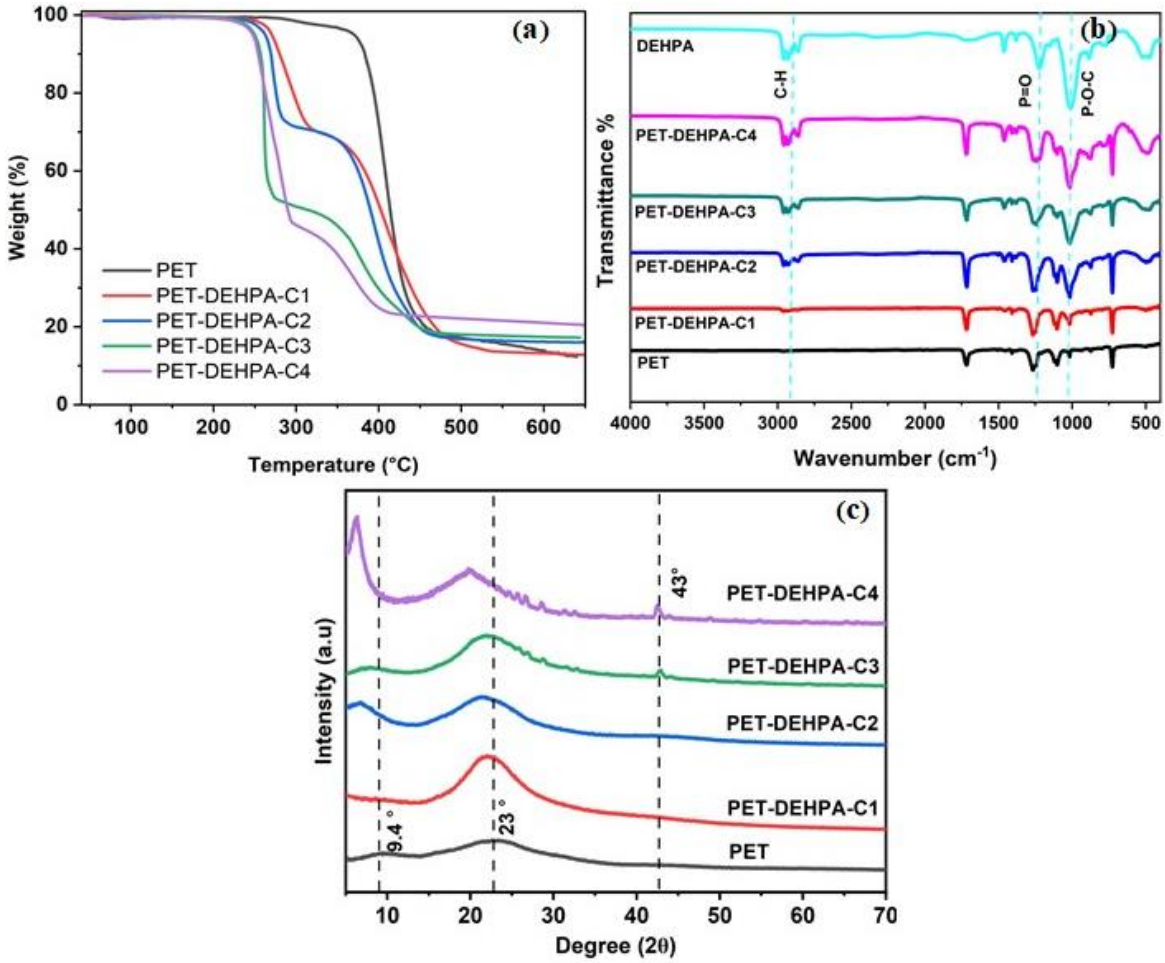

Figure 3: Thermographs profiles (a), Chemical bonding (b) and diffraction patterns (c) of pristine PET and PET nanofibers modified with DEHPA at 5 wt% (C1), 10 wt% (C2), 15 wt% (C3), 20 wt% (C4).

Furthermore, the weight percentage losses of DEHPA ligand increased from 1.5 mg for PET-DEHPA-C1 (5 wt%) to the highest amount of 2.7 mg for PET-DEHPA-C4 (20 wt%) nanofibers. This observation supports the SEM images where the crosslinking of nanofibers was observed thus changing the initial fibrous structure of PET nanofibers. TGA results support the XPS analysis which showed that as the DEHPA concentration was increased so was the content (%) of P in the nanofibers. Further chemical analysis was performed using FTIR-ATR. On the other hand, PET (2.8 mg) content in the PET-DEHPA nanofibers was the highest when the least amount of DEHPA ligand (5 wt%) was present but the amount decreased as the amount of DEHPA increased and the lowest was observed on the PET-DEHPA-C4 (20 wt%) nanofibers with a mass of 1.2 mg. Overall, this weight of losses observed were relatively low for PET modified with DEHPA ligand and seemed to be dependent with the ligand. For instance, Ahmed et al. (2021) observed that PET nanofibers exhibited a weight loss of 79.01 % at 454.57 °C, whereas the weight loss of 56.84 % for modified PET-dibenzo-18-crown-6 nanofibers occurred at 464.13 °C. Nevertheless, the presence of the two distinguishable degradation steps in Fig. 3a implied that the bound DEHPA ligand exhibited thermal stability and maintained its structural integrity up to 230 °C as also reported by Yadav et al. (2013). Therefore, the PET-DEHPA nanofibers can be used for recovery of metal ions at temperatures below 230 ºC. To assess

further potential of the fabricated PET-DEHPA nanofibers it was imperative to identify the types of functional groups. In Fig. 3b the FTIR spectra of pristine PET compared with that of PET-DEHPA nanofibers showed that additional peaks were observed on the PET-DEHPA nanofiber spectra. The additional peaks which are characteristic of DEHPA were observed at 1010 cm^{-1}, 1239 cm^{-1} and a multi-peak at about 2900 cm^{-1}. The three peaks were attributed to P-O-C, P=O and C-H, respectively. The P=O peak overlapped with the C=O peak from the PET compound thus showing a broad peak. These IR peaks of PET and modified PET-DEHPA nanofibers were in good agreement with peaks reported by Ahmed et al. (2021) and Chen et al. (2013). Structural ordering of pristine PET and modified PET nanofibers as shown in Fig. 3c further shows that the pristine PET nanofibers were amorphous, while the modified PET-DEHPA nanofibers exhibited increased peak intensities roughly at 2θ: 9 ° and 2θ: 23 °. The characteristic broad peaks of PET were consistent with the reported diffractogram of PET (Pereao et al. 2021). However, the PET-DEHPA peaks notably shifted to lower 2θ values with increase in intensities compared to pristine PET. This peak shifting and increase was proportional to the increase in DEHPA ligand concentration. The increase in peak intensity is an indication that the fabricated PET-DEHPA nanofibers were structurally ordered (Chen et al. 2013). Sharp peaks observed on the broad peak at about 2θ: 23 ° on the PET-DEHPA-C3&C4 diffractograms further implied that the fabricated nanofibers displayed long-range ordering (Li et al.2018). In addition, the diffractograms of PET-DEHPA- C3 & C4 had additional weak but distinct peaks at 2θ: 43 ° and other small peaks were apparent on the main broad peak at 2θ: 23 °. Furthermore, the peak at 2θ: 8 ° on the PET-DEHPA-C4 diffractogram demonstrated a significant increase in intensity and sharpness, showing greater long-range ordering compared to the peak at 2θ: 9.4 ° on the pristine PET diffractogram.

1.2.3 Methodology and Results: Batch adsorption

Batch adsorption was carried out in various concentrations (20 – 120 mg/L) of synthetic solutions of Co, Ni and Mn metal ions. The pH of the solutions was investigated between 2 – 6 values and solutions were adjusted with HNO_3 and NaOH. The kinetic study was investigated using 20 – 30 mg of the electrospun nanofibers in the range of 5 – 180 min. A Promax 1020 (Heidolph) shaker was used while set at a speed of 80 rpm. The selectivity of the PET-DEHPA adsorbent towards Mn ion was assessed using competitive batch adsorption experiments in the presence of C_o and Ni, interfering ions. Table 2 shows different sets of metal ion concentrations used in the competitive experiments. Equation 1 was used to calculate the recovered efficiency (% Recovery) of the metal cations. Where C_o and Ce are the initial and equilibrium concentrations (mg/L) of metal ions in the solution, respectively. The PET-DEHPA nanofibers were tested for chemical stability of the modified PET-DEHPA nanofibers was conducted in 0.1 – 2.0 M HNO_3 acid. The PET-DEHPA nanofiber was air-dried overnight then analyzed using FTIR-ATR.

Table 2: The preparation of the solution mixtures of metal ions.

Fractions	Co (mg/L)	Ni (mg/L)	Mn (mg/L)
1:2:2	20	40	40
2:1:2	40	20	40
2:2:1	40	40	20

$$\% \text{ Recovery} = [(C_o - C_t)/C_o] * 100 \quad (1)$$

Where Co and Ct are the metal cation initial and final concentrations, respectively.

Fig. 4a shows the adsorption trends of Ni, Co, or Mn metal ions using PET electrospun nanofibers modified with 5 wt% (C1), 10 wt% (C2) and 15 wt% (C3) of DEHPA ligand. It was found that pristine PET nanofibers absorbed less than 3 % of Ni or Co and about 7 % of Mn. Nonetheless, pristine nanofibers had the least metal ion adsorption capacity compared to all the modified PET-DEHPA nanofibers. Notably, as the used concentration of DEHPA chelating ligand increased, so did the adsorption capacity of the modified adsorbent. The highest concentration of DEHPA ligand (C3, 15 %) resulted in the highest adsorption of about 9 % Ni, 13% Co and 35 % Mn. This adsorption trend showed that the DEHPA ligand improved the adsorption capacity of pristine PET and PET-DEHPA-C3 (15 %) had a higher affinity towards Mn ion thus was selected to be used for further adsorption experiments.

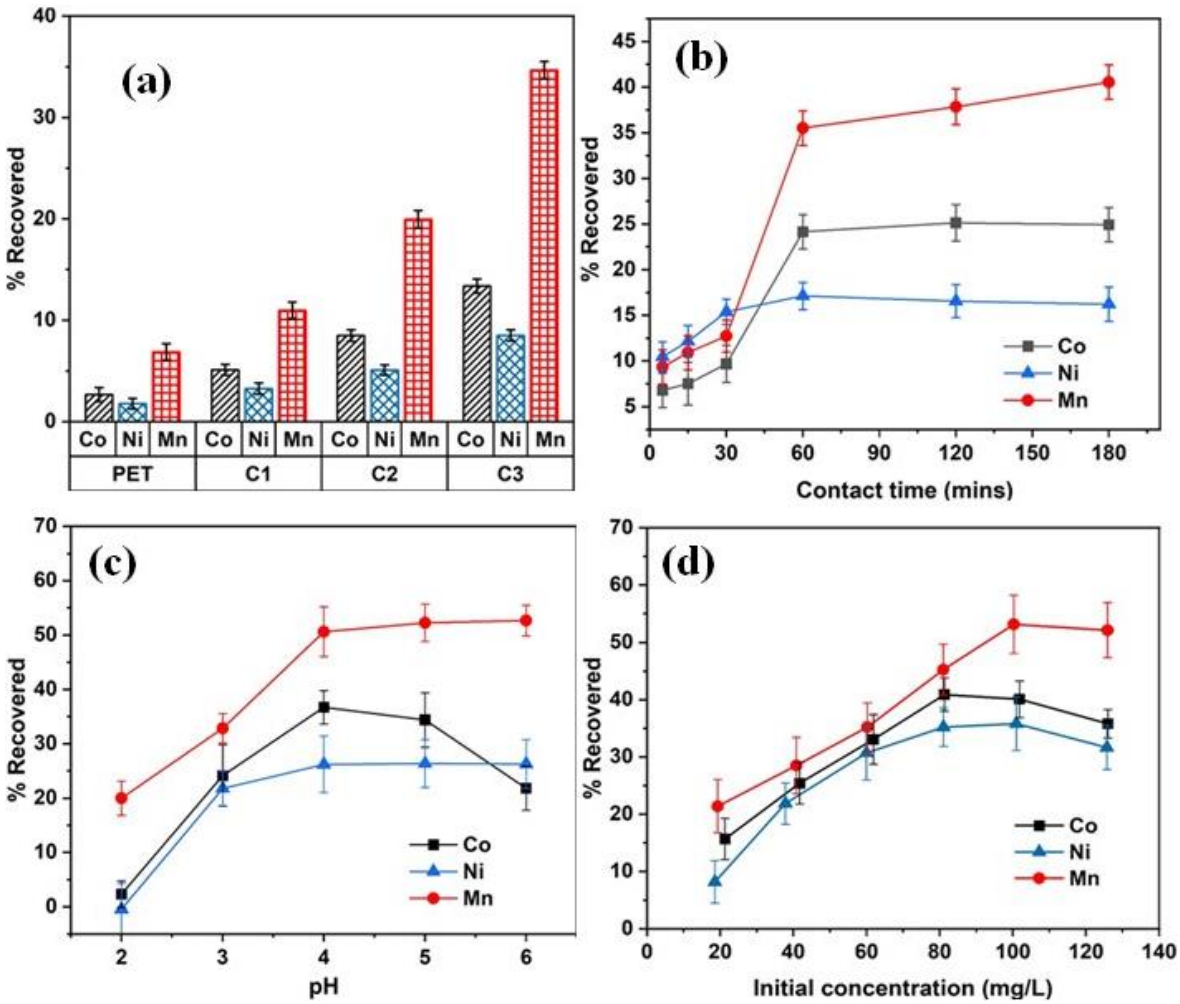

Figure 4: Effect of (a) DEHPA concentration (wt%), (b) contact time (min) (c) solution pH, (d) initial concentration (mg/L).

The kinetic study as shown in Fig. 4b revealed that at the initial stage (5 – 30 mins), ions selectively occupied active sites on the nanofibers and as the contact time increased, the available active sites decreased. This was demonstrated by the plateau on the plots from 60 to 180 mins (Fig. 4b). This kinetic trend was in correlation to that reported by Pereao et al. (2017). It was further observed that all the three metals reached their adsorption equilibrium from 60

mins. For the first 30 mins, Ni ion was the most absorbed with an adsorption recovery of about 15 % while it was 7.5 % Co and 12.7 % Mn. However, above 30 mins the recovery percentages of both Co and Mn ions increased with their highest reaching 25% and 41%, respectively while Ni ion was the least adsorbed (16 %). The solution pH is one of the key parameters that influence the adsorption of metal ions as it involves the protonation and deprotonation of the chelating ligands (Chen et al. 2013). Thus, as shown in Fig. 4c at lowest pH 2, the adsorption capacity was the least percentage (i.e., ~5% (Ni or Co) and 20 % Mn) and this was attributed to the competitive influence of prevalent protons (H^+) ions. As the pH increased from 3, the adsorption capacity also increased which was due to the decrease in the available protons. Mn ion was the most adsorbed with the highest recovery of 53 %, followed by Co (37 %) then Ni (26 %) being the least. This increase in adsorption capacity at high pH values especially for Co and Mn ions was due to the availability of more accessible active sites as the degree of protonation of the surface functional groups gradually decreased.

From pH 4 and above, the adsorption plots of all the three ions reached equilibrium thus, pH 4 was selected for further experiments in the study. A similar trend was also reported by Morillo Martí et al. (2017) and Pereao et al. (2021). However, when Islam et al. (2015) used functionalized phosphine Poly (vinyl alcohol)/ silicon dioxide (p-PVA/SiO_2) composite nanofiber adsorbent to recover Ni and Mn ions, they observed an increasing adsorption trend which reached equilibrium at pH 6. Thus, opposing the adsorption trends in this study. The observed differences may be due to several factors such as the degree of protonation of the ligands and polymer supports (Hu et al. 2018). In overall, pH 4 was selected for further adsorption experiments as a suitable pH for all the metal ions. Fig. 4d shows that with the increase in the initial metal ions concentration above 80 mg/L, the available adsorption sites on the surface of the PET-DEHPA nanofibers reached saturation. Thus, signifying equilibrium in the adsorption-desorption dynamics. PET-DEHPA nanofibers demonstrated a higher affinity towards Mn, followed by Co and Ni ions as the least adsorbed. Notably, Ni, Co and Mn metal ions reached the adsorption plateau between 80 and 100 mg/L. However, the maximum adsorption capacities of Ni, Co and Mn ions were 32 %, 41 % and 54 %, respectively. This behaviour aligned with specific adsorption processes wherein the adsorption rate was primarily influenced by the availability of accessible adsorption sites on the adsorbent surface, without diffusional constraints (Pereao et al. 2021).

1.2.4 Methodology and Results: Selectivity of metal ions

Since Mn ion was the most adsorbed in all single adsorption system as discussed in Fig. 5, a competitive metal ion adsorption experiment involving Ni and Co as interfering metal ions was conducted to determine the selectivity of PET-DEHPA nanofibers towards Mn. Fig. 5a showed that Mn ion (58 %) remained as the most adsorbed ion compared to Ni (5 %) and Co (11 %) ions in the first mixture where equal metal ion concentrations were used. Even after the solution mixture ratios were varied while keeping the concentration of Mn ion the least, it remained the most adsorbed ion. The recovery capacities of Ni, Co and Mn were approximately 8 %, 13% and 47 %, respectively, thus confirming the specific selectivity of PET-DEHPA nanofiber adsorbent towards Mn ion. This selectivity capability towards Mn ion was attributed to the good chemical stability of the metal ion complex with the functional groups of the chelating DEHPA ligand. Furthermore, according to the Pearson's theory, Mn is a hard acid, and it is prone to strongly coordinate with hard bases which typically contain oxygen species such as PO_4^{3-} (which is present in DEHPA ligand). While the other interfering metal ions (i.e., Ni and

Co) are categorized as borderline acids hence they were insignificantly adsorbed in the presence of Mn ion (Hu et al. 2018). Therefore, PET-DEHPA nanofiber adsorbent has the potential to be useful in the process of selective separation and recovery of the valuable metals from the spent LIBs.

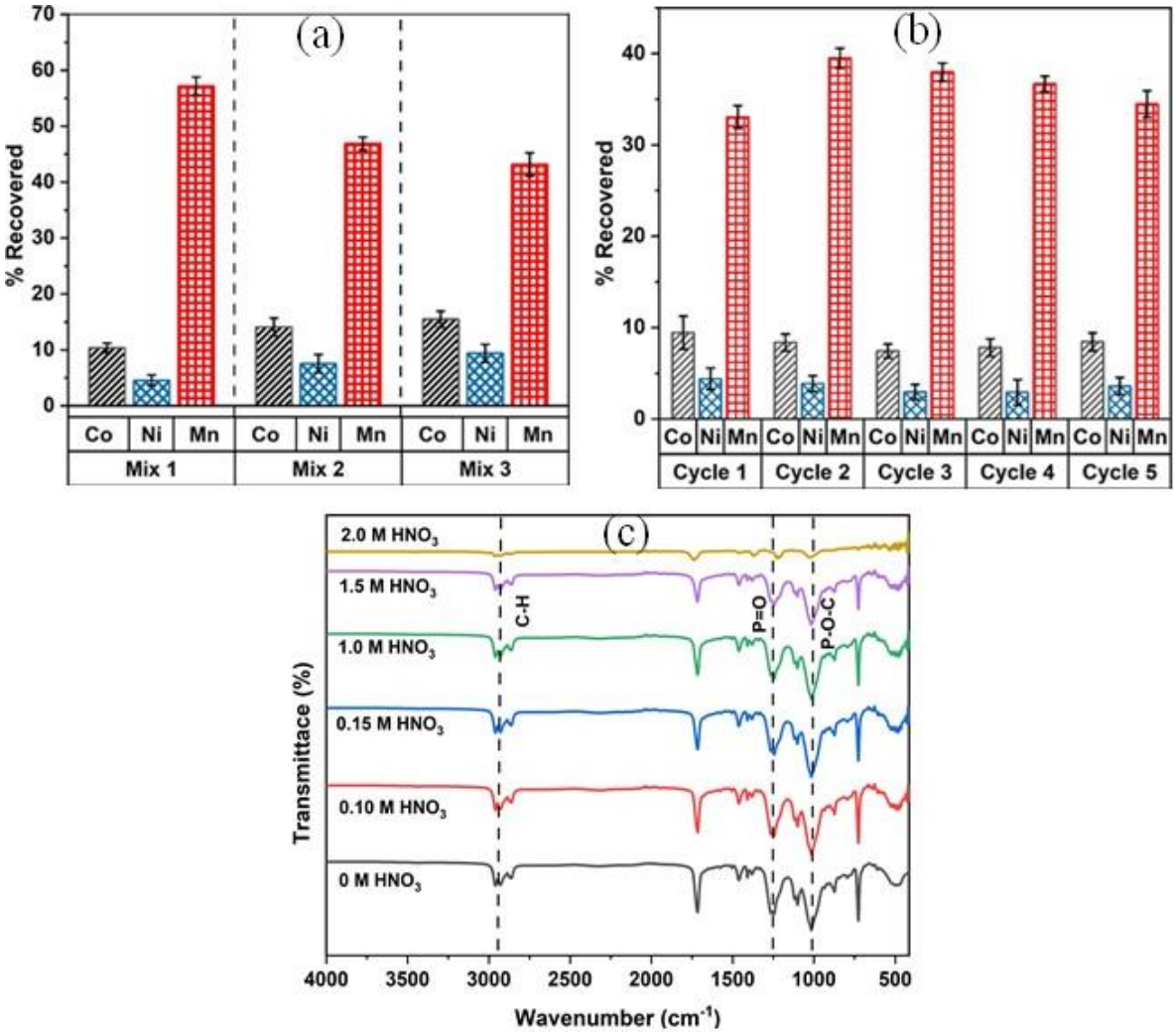

Figure 5: Selectivity of metal cations (a), regeneration of adsorbent nanofibers (b), and IR spectra of nanofibers after stability test in HNO_3 solutions.

Fig. 5b further revealed that PET-DEHPA exhibited relatively consistent adsorption capacities over five cycles. Ni, Co, and Mn metal ions were relatively recovered at percentages of about 5 %, 11% and 41 %, respectively. Notably, the adsorption trend over the five cycles did not show any significant loss in the initial (cycle 1) binding affinity of the adsorbent towards the targeted metal ions. Interestingly, the regeneration results further supported the selectivity results which showed that PET-DEHPA had a higher binding affinity towards Mn, even in the presence of Ni and Co interfering ions. The chemical stability of PET-DEHPA-C3 (15 %) as shown in Fig. 5c also revealed that the prominent peaks attributed to P-O-C, P = O and C-H at 1010 cm^{-1}, 1250 cm^{-1} and 2950 cm^{-1} respectively, did not change in either their intensities or wavenumbers after exposure to HNO_3 acid at concentrations between 0.1 M to 1.5 M. This implied that PET-DEHPA-C3 (15 %) nanofiber adsorbent was chemically stable up to a concentration of 1.5 M HNO_3 acid.

However, a decrease in the three prominent peak intensities was observed after exposure to a higher concentration of 2.0 M HNO_3 acid.

1.2.5 Conclusions

This study synthesized electrospun polyethylene terephthalate (PET) nanofiber adsorbent and modified the surface with Di-2-ethylhexyl phosphoric acid (DEHPA) to recover metal ions (Ni, Co, or Mn) from spent lithium-ion batteries (LIB) cathode materials. The PET-DEHPA was characterized by SEM, EDS, FTIR, XPS, TGA, and XRD and used for the adsorption of valuable metals such as Ni, Co, and Mn ions which are primarily found in the cathode material of spent lithium-ion batteries. The optimal conditions for the adsorption of Ni, Co, and Mn ions solution were determined at pH 4, 60 mins contact time, and initial metal ion concentrations of 100 mg/L. Mn ion has a recovery efficiency of 57% compared to Ni (7%) and Co (13%). The adsorption kinetics of Mn was achieved within 60 mins and was selective over interfering ions such as Ni and Co. PET-DEHPA nanofiber adsorbent demonstrated excellent regeneration capability over 5 cycles. The regeneration of the developed PET-DEHPA nanofiber adsorbent and its selective recovery of Mn ions underscore the potential for sustainable and cost-effective metal recovery from spent LIBs.

2 Research Outputs

The research work yielded the following publications;

1. Tawonezvi, T., Nomnqa, M., Petrik, L. & Bladergroen, B.J. 2023. Recovery and Recycling of Valuable Metals from Spent Lithium-Ion Batteries: A Comprehensive Review and Analysis. Journal of Energies (MDPI).

Abstract:

The recycling of spent lithium-ion batteries (Li-ion Batteries) has drawn a lot of interest in recent years in response to the rising demand for the corresponding high-value metals and materials and the mounting concern emanating from the detrimental environmental effects imposed by the conventional disposal of solid battery waste. Numerous studies have been conducted on the topic of recycling used Li-ion batteries to produce either battery materials or specific chemical, metal or metal-based compounds. Physical pre-treatment is typically used to separate waste materials into various streams, facilitating the effective recovery of components in subsequent processing. In order to further prepare the recovered materials or compounds by applying the principles of materials chemistry and engineering, a metallurgical process is then utilized to extract and isolate pure metals or separate contaminants from a particular waste stream. In this review, the current state of spent Li-ion battery recycling is outlined, reviewed, and analyzed in the context of the entire recycling process, with a particular emphasis on hydrometallurgy; however, electrometallurgy and pyrometallurgy are also comprehensively reviewed. In addition to the comprehensive review of various hydrometallurgical processes, including alkaline leaching, acidic leaching, solvent (liquid liquid) extraction, and chemical precipitation, a critical analysis of the current obstacles to process optimization during Li-ion battery recycling is also conducted. Moreover, the energy-intensive nature of discussed recycling process routes is also assessed and addressed. This

study is anticipated to offer recommendations for enhancing wasted Li-ion battery recycling, and the field can be further explored for commercialization.

2. Tawonezvi, T., Nomnqa, M., Zide D., Petrik, L. & Bladergroen, B.J. 2023. Selective electrodeposition of Co-Ni alloys from synthetic quasi–LiB NMC 532 cathode sulphate solutions using rotating plate potentiostatic electrowinning. Chemical Engineering Journal Advances (Elsevier).

Abstract:
The interest in recycling spent lithium-ion batteries (Li-ionB) has surged due to the rising demand for valuable metals (e.g., Co, Ni, Li and Mn) and concerns about environmental repercussions emanating from conventional battery waste disposal. This research is centered on the recovery of the valuable Ni-Co alloys from synthetic Ni, Co, Mn and Li sulphate solutions mimicking the NMC 532 ratio of elements using a hydro-electrometallurgy process route that integrates hydrometallurgy and potentiostatic electrometallurgy techniques. This quasi-model is done to elucidate the effect of multiple influencing parameters, through isolation and varying, on the selective electrodeposition of Co-Ni from multi-ion (Li, Ni, Mn and Co) complex solutions before applying it using real cathode leachates. The selective electrowinning metal recovery process route is a cost-effective alternative to the energy, cost and material-intensive hydrometallurgy intermediate purification processes such as solvent extraction, selective precipitation, and ion-exchange. The study delves into the effects of various electrowinning parameters, including applied potential, temperature, pH, Co, Ni, Na_2SO_4, NaH_2PO_4 buffer concentration, and cathode rotational speed. These parameters were thoroughly investigated and effectively optimised to achieve the recovery of 98.2% pure $Ni_{0.65}Co_{0.35}$ at a rate of 0.060 g/cm^2.h with an impressive 89.25 % current efficiency. The composition of the electrowon deposit was meticulously quantified using Inductively Coupled Plasma Optical Emission Spectroscopy (ICP-OES) and subjected to analysis through a Scanning Electron Microscope (SEM-EDS). Additionally, the phase composition was evaluated using X-Ray Diffraction analysis (XRD). The results successfully demonstrate the technical feasibility of recovering Ni-Co alloys, yielding high quantities of industrial-grade pure Ni-Co alloys. This comprehensive electro-hydrometallurgical process, designed for both closed and loop recycling purposes, promotes a more environmentally preservative approach to recycling spent lithium-ion battery cathode material. The approach contributes significantly to the development of sustainable resource management infrastructure.

3. Tawonezvi, T., Zide, D., Nomnqa, M., Madondo, M., Petrik, L. & Bladergroen, B.J. 2023. Recovery of NixMnyCoz $(OH)_2$ and Li_2CO_3 from Spent Lithium-Ion Battery Cathodes through Non-Na Precipitant-Based Chemical Precipitation for Sustainable Recycling. Chemical Engineering Journal Advances (Elsevier).

Abstract:

The interest in recycling spent lithium-ion batteries (Li-ionB) has surged due to the rising demand for valuable metals (e.g., Co, Ni, Li and Mn) and concerns about environmental repercussions emanating from conventional battery waste disposal. Conventional precipitation-based hydrometallurgy recycling processes utilise Na-based or metal-based precipitants. The Na, from Na-based precipitants, is present in high concentrations in the

process effluent since they are not recovered during the recycling process. The Na-rich effluent cannot be discarded since it doesn't meet environmental regulations as per the U.S. Environmental Protection Agency (EPA) (2023) therefore creating a storage and disposal problem. It is therefore imperative to utilise non-Na-based precipitants to eliminate the effluent disposal problem. This paper focuses on the recovery of $Ni_xCo_yMn_z(OH)_2$ and Li_2CO_3, main precursors for Li-ionB cathode production, from a typical spent Li-ionB cathode (NMC 532) using non-Na precipitant-based chemical precipitation. This study reports $Ni_xCo_yMn_z(OH)_2$ and Li_2CO_3 recovery from spent Li-ionBs for closed-loop Li-ionB cathode recycling through an integrated hydrometallurgy and chemical precipitation process. Through the utilisation of leachate solutions comprising 2 M H_2SO_4 + 6 vol.% H_2O_2, and a 75 g/L S/L ratio and conducting leaching for 120 min at a temperature of 60 °C and IS of 350 rpm, the recovery efficiency of 98.1 % for Li, 97.1 % for Co, 96.1 % for Ni, and 95.7 % for Mn. The pH of the NMC leachate was initially adjusted to 5 to precipitate Fe, Al and Cu impurities. Thereafter, active metal species (Ni, Mn and Co) were precipitated at a pH of 13 as $Ni_{0.5}Co_{0.2}Mn_{0.3}(OH)_2$ composite microparticles by adding LiOH precipitant. Thereafter, the Li-rich resultant liquor was further used to recover the Li by adding 3.4 mol of CO_2 bubbled at 0.068 mol (CO_2)/L.min and 40 °C for 45 min. The Li_2CO_3 precipitates were separated from the suspension through filtration followed by washing using deionised water and hot air drying. The reaction time is 45 mins, and the agitation speed is 150 rpm. Through this multi-stage precipitation process, >98 % of Ni, Co, Mn and > 91 % of Li can be recovered in the form of $Ni_{0.5}Mn_{0.3}Co_{0.2}OH_2$ and Li_2CO_3 respectively. The process exhibits great potential for recovery of valuable materials from spent Li-ionBs. The recovered $Ni_{0.5}Co_{0.2}Mn_{0.3}(OH)_2$ and Li_2CO_3 materials will be used as precursors in the anhydrous NMC cathode production process.

The research work yielded the following conference and seminar presentations;

Type of outputs	Author(s)	Title	Status [6] (Draft/ Final)	Date presented (month/year)	Final deliverable provided to CSIR (Yes/No)
Conference papers and presentation	J. Mukaba, O. Pereao, B.J. Bladergroen, and L. Petrik	New improved nanofiber material for the recovery of metals from spent lithium-ion batteries	Presented	Aug 2022	Yes
Seminar	L.Petrik, T. Tawonezvi, D Zide, BJ Bladergroen, G Ndayambaje, T. Totito	Batteries' Waste Management	Presented	Oct 2023	Yes
Local Symposium Presentation	Madondo, M., Zide, D., Tawonezvi, T. & Bladergroen, B. J	The Recovery of Nickel, Manganese, Cobalt, and Lithium from Spent Lithium-Ion Batteries by Chemical Precipitation	presented (Presentation won 3rd best presentation)	Nov 2023	Yes
	Dyonashe, N., Zide, D., Tawonezvi, T. & Bladergroen, B. J	Leaching optimization NMC cathode material using organic acid and reducing agent to recover valuabl	Presented	Nov 2023	Yes
Mini Thesis	Madondo, M., Zide, D., Tawonezvi, T. & Bladergroen, B.J	The Recovery of Nickel, Manganese, Cobalt, and Lithium from Spent Lithium-Ion Batteries by Chemical Precipitation	Submitted to CPUT and assessed	Nov 2023	Yes
	Dyonashe, N., Zide, D., Tawonezvi, T. & Bladergroen, B.J	Leaching optimization NMC cathode material using organic acid and reducing agent to recover valuable metals from spent Li-ion batteries	Submitted to CPUT and assessed	Nov 2023	Yes

3 References

- ESMAP. 2022. Reuse and Recycling: Environmental Sustainability of Lithium-Ion Battery Energy Storage Systems An Energy Storage Partnership Report. www.worldbank.org.
- Njema, G.G., Ouma, R.B. and Kibet, J.K. (2024) 'A review on the recent advances in battery development and Energy Storage Technologies', *Journal of Renewable Energy*, 2024, pp. 1–35. doi:10.1155/2024/2329261.
- Liu, C., Neale, Z.G. and Cao, G. (2016) 'Understanding electrochemical potentials of cathode materials in rechargeable batteries', *Materials Today*, 19(2), pp. 109–123. doi:10.1016/j.mattod.2015.10.009.
- Milian, Y.E. *et al.* (2024) 'A comprehensive review of emerging technologies for recycling spent lithium-ion batteries', *Science of The Total Environment*, 910, p. 168543. doi:10.1016/j.scitotenv.2023.168543.
- Tawonezvi, T. *et al.* (2024a) 'Selective electrodeposition of co-ni alloys from synthetic quasi lib NMC 532 cathode sulphate solutions using rotating plate potentiostatic electrowinning', *Chemical Engineering Journal Advances*, 17, p. 100579. doi:10.1016/j.ceja.2023.100579.
- T. Tawonezvi, M. Nomnqa, L. Petrik, and B. J. Bladergroen, "Recovery and Recycling of Valuable Metals from Spent Lithium-Ion Batteries: A Comprehensive Review and Analysis," *Energies (Basel)*, vol. 16, no. 3, p. 1365, Jan. 2023, doi: 10.3390/en16031365.
- X. Zeng, J. Li, and Y. Ren, "Prediction of various discarded lithium batteries in China," in *2012 IEEE International Symposium on Sustainable Systems and Technology (ISSST)*, IEEE, May 2012, pp. 1–4. doi: 10.1109/ISSST.2012.6228021.
- X. Zheng *et al.*, "A Mini-Review on Metal Recycling from Spent Lithium-Ion Batteries," *Engineering*, vol. 4, no. 3, pp. 361–370, Jun. 2018, doi: 10.1016/j.eng.2018.05.018.
- W.-S. Chen and H.-J. Ho, "Recovery of Valuable Metals from Lithium-Ion Batteries NMC Cathode Waste Materials by Hydrometallurgical Methods," *Metals (Basel)*, vol. 8, no. 5, p. 321, May 2018, doi: 10.3390/met8050321.
- S. J. Gao, W. F. Liu, D. J. Fu, and X. G. Liu, "Research progress on recovering the components of spent Li-ion batteries," *New Carbon Materials*, vol. 37, no. 3, pp. 435–460, Jun. 2022, doi: 10.1016/S1872-5805(22)60605-X.
- E. des Ligneris, L. F. Dumée, and L. Kong, "Nanofibers for heavy metal ion adsorption: Correlating surface properties to adsorption performance, and strategies for ion selectivity and recovery," *Environ Nanotechnol Monit Manag*, vol. 13, p. 100297, May 2020, doi: 10.1016/j.enmm.2020.100297.
- N. Bhardwaj and S. C. Kundu, "Electrospinning: A fascinating fiber fabrication technique," *Biotechnol Adv*, vol. 28, no. 3, pp. 325–347, May 2010, doi: 10.1016/j.biotechadv.2010.01.004.
- T. C. Totito, K. Laatikainen, O. Pereao, C. Bode-Aluko, and L. Petrik, "Adsorptive Recovery of Cu2+ from Aqueous Solution by Polyethylene Terephthalate Nanofibres Modified with 2-(Aminomethyl) Pyridine," *Applied sciences*, vol. 11, no. 24, p. 11912, 2021, doi: 10.3390/app112411912.
- M. Khorram, A. Mousavi, and N. Mehranbod, "Chromium removal using adsorptive membranes composed of electrospun plasma-treated functionalized polyethylene terephthalate (PET) with chitosan," *J Environ Chem Eng*, vol. 5, no. 3, pp. 2366–2377, Jun. 2017, doi: 10.1016/j.jece.2017.04.010.
- B. M. Thamer, A. Aldalbahi, M. Moydeen A, A. M. Al-Enizi, H. El-Hamshary, and M. H. El-Newehy, "Fabrication of functionalized electrospun carbon nanofibers for enhancing lead-ion adsorption from aqueous solutions," *Sci Rep*, vol. 9, no. 1, p. 19467, Dec. 2019, doi: 10.1038/s41598-019-55679-6.
- J. A. Abbas, I. A. Said, M. A. Mohamed, S. A. Yasin, Z. A. Ali, and I. H. Ahmed, "Electrospinning of polyethylene terephthalate (PET) nanofibers: optimization study using taguchi design of experiment," *IOP Conf Ser Mater Sci Eng*, vol. 454, p. 012130, Dec. 2018, doi: 10.1088/1757-899X/454/1/012130.
- S. Yasin, Z. H. Bakr, G. A. M. Ali, and I. Saeed, "Recycling Nanofibers from Polyethylene Terephthalate Waste Using Electrospinning Technique," 2021, pp. 805–821. doi: 10.1007/978-3-030-68031-2_28.

- D. Morillo Martín, M. Magdi Ahmed, M. Rodríguez, M. García, and M. Faccini, "Aminated Polyethylene Terephthalate (PET) Nanofibers for the Selective Removal of Pb (II) from Polluted Water," *Materials*, vol. 10, no. 12, p. 1352, Nov. 2017, doi: 10.3390/ma10121352.
- O. K. Pereao, K. Laatikainen, C. Bode-Aluko, O. Fatoba, E. Omoniyi, Y. Kochnev, A. N. Nechaev, P. Apel, and L. Petrik, "Synthesis and characterization of diglycolic acid functionalized polyethylene terephthalate nanofibers for rare earth elements recovery," *J Environ Chem Eng*, vol. 9, no. 5, Oct. 2021, doi: 10.1016/j.jece.2021.105902.
- F. Nunes da Silva, M. M. Bassaco, D. A. Bertuol, and E. H. Tanabe, "An eco-friendly approach for metals extraction using polymeric nanofibers modified with di-(2-ethylhexyl) phosphoric acid (DEHPA)," *J Clean Prod*, vol. 210, pp. 786–794, 2019, doi: 10.1016/j.jclepro.2018.11.098.
- W.-S. Chen and H.-J. Ho, "Recovery of Valuable Metals from Lithium-Ion Batteries NMC Cathode Waste Materials by Hydrometallurgical Methods," *Metals (Basel)*, vol. 8, no. 5, p. 321, May 2018, doi: 10.3390/met8050321.
- B. Tarus, N. Fadel, A. Al-Oufy, and M. El-Messiry, "Effect of polymer concentration on the morphology and mechanical characteristics of electrospun cellulose acetate and poly (vinyl chloride) nanofiber mats," *Alexandria Engineering Journal*, vol. 55, no. 3, pp. 2975–2984, Sep. 2016, doi: 10.1016/j.aej.2016.04.025.
- A.-H. Chen, S.-C. Liu, C.-Y. Chen, and C.-Y. Chen, "Comparative adsorption of Cu (II), Zn (II), and Pb (II) ions in aqueous solution on the crosslinked chitosan with epichlorohydrin," *J Hazard Mater*, vol. 154, no. 1–3, pp. 184–191, Jun. 2008, doi: 10.1016/j.jhazmat.2007.10.009.
- K. K. Singh, S. K. Pathak, M. Kumar, A. K. Mahtele, S. C. Tripathi, and P. N. Bajaj, "Study of uranium sorption using D2EHPA-impregnated polymeric beads," *J Appl Polym Sci*, vol. 130, no. 5, pp. 3355–3364, Dec. 2013, doi: 10.1002/app.39582.
- K. K. Yadav, D. K. Singh, M. Anitha, L. Varshney, and H. Singh, "Studies on separation of rare earths from aqueous media by polyethersulfone beads containing D2EHPA as extractant," *Sep Purif Technol*, vol. 118, pp. 350–358, Oct. 2013, doi: 10.1016/j.seppur.2013.07.012.
- H. A. Ahmed, P. H. Saleem, S. A. Yasin, and I. A. Saeed, "The application of modified polyetheleneterephthalate (PET) nanofibers; characterization and isotherm study," *J Phys Conf Ser*, vol. 1853, no. 1, p. 012006, Mar. 2021, doi: 10.1088/1742-6596/1853/1/012006.
- Z. Chen, J. N. Hay, and M. J. Jenkins, "The thermal analysis of poly (ethylene terephthalate) by FTIR spectroscopy," *Thermochim Acta*, vol. 552, pp. 123–130, Jan. 2013, doi: 10.1016/j.tca.2012.11.002.
- Tabatabaeefar, A. R. Keshtkar, and M. A. Moosavian, "Preparation and characterization of a novel electrospun ammonium molybdophosphate/polyacrylonitrile nanofiber adsorbent for cesium removal," *J Radioanal Nucl Chem*, vol. 305, no. 2, pp. 653–664, Aug. 2015, doi: 10.1007/s10967-015-3973-0.
- M. Li, X. Tian, R. Jin, and D. Li, "Preparation and characterization of nanocomposite films containing starch and cellulose nanofibers," *Ind Crops Prod*, vol. 123, pp. 654–660, Nov. 2018, doi: 10.1016/j.indcrop.2018.07.043.
- O. K. Pereao, C. Bode-Aluko, G. Ndayambaje, O. Fatoba, and L. F. Petrik, "Electrospinning: Polymer Nanofibre Adsorbent Applications for Metal Ion Removal," *J Polym Environ*, vol. 25, no. 4, pp. 1175–1189, Dec. 2017, doi: 10.1007/s10924-016-0896-y.
- Md. S. Islam, Md. S. Rahaman, and J. H. Yeum, "Phosphine-functionalized electrospun poly (vinyl alcohol)/silica nanofibers as highly effective adsorbent for removal of aqueous manganese and nickel ions," *Colloids Surf A Physicochem Eng Asp*, vol. 484, pp. 9–18, Nov. 2015, doi: 10.1016/j.colsurfa.2015.07.023.
- H. Hu, H. He, J. Zhang, X. Hou, and P. Wu, "Optical sensing at the nanobiointerface of metal ion–optically-active nanocrystals," *Nanoscale*, vol. 10, no. 11, pp. 5035–5046, 2018, doi: 10.1039/C8NR00350E.

ANNEXURE 1

TITLE – IF ANNEXURES ARE NEEDED FOR SUPPORTING DOCUMENTATION

Council for Scientific and Industrial Research

Waste RDI Roadmap Implementation Unit

Meiring Naudé Road, Brummeria,
Pretoria, South Africa

Postal Address

PO Box 395, Pretoria, South Africa, 0001

Tel: +27 (0)12 841 4801
Fax: +27 (0)12 842 7687
Email: info@wasteroadmap.co.za

www.wasteroadmap.co.za

Department of Science and Innovation

Directorate: Environmental Services and Technologies

Meiring Naudé Road, Brummeria,
Pretoria, South Africa

Postal Address

Private Bag X894, Pretoria, South Africa, 0001

Tel: +27 (0)12 843 6300

www.dst.gov.za